Solution Structures of Two Structural Isoforms of CMrVIA χ/λ-Conotoxin

Tse Siang Kang,[†] Seetharama D. S. Jois,[‡,§] and R. Manjunatha Kini*[,†]

Protein Science Laboratory, Department of Biological Sciences, National University of Singapore, 14 Science Drive 4, Block S3 #03-17 Singapore 117543, and Department of Pharmacy, National University of Singapore, Singapore 117543

Received March 21, 2006; Revised Manuscript Received May 23, 2006

α-Conotoxins possess a conserved four-cysteine framework and disulfide linkages (C_{1-3}, C_{2-4}) that fold toward the globular conformation with absolute fidelity. Despite the presence of a similar conserved set of cysteine framework, χ/λ-conotoxins adopt an alternate disulfide-pairing (C_{1-4}, C_{2-3}) and its consequent ribbon conformation, exhibiting distinct biological activities from α-conotoxins. χ/λ-Conotoxin CMrVIA (VCCGYKLCHOC-*COOH*) isolated from the venom of *Conus marmoreus* natively exists in the ribbon conformation and induces seizures in mice at a potency that is of three orders higher than the non-native globular form. We have chemically synthesized two isoforms of CMrVIA conotoxin in the ribbon and globular conformation and determined their structures by ^{1}H NMR spectroscopy. The ribbon (PDB ID 2B5P) and globular conformations (PBD ID 2B5Q) were calculated to have paired-wise backbone RMSDs of 0.48 ± 0.1 and 0.58 ± 0.1 Å respectively. Unlike the native globular α-conotoxins, the globular canonical form of CMrVIA χ/λ-conotoxin exhibited heterogeneity in its solution structure as noted by the presence of minor conformers and poorer RMSD of structure calculation. Paired-wise backbone comparison between the native ribbon and the non-native globular form of CMrVIA conotoxin revealed an RMSD of 4.73 Å, emphasizing their distinct conformational differences. These structural data are essential for the understanding of the structure−function activity of χ/λ-conotoxins, as well as unraveling the folding propensities of these short peptide toxins.

Introduction

The venom of the marine predatory cone snails contains a plethora of peptide toxins of exceptional specificity and potency. In general, these peptide toxins, collectively termed as conotoxins, are small in size and predominantly rich in cysteine residues. On the basis of the conserved cysteine framework and biological activities, these conotoxins are classified into several superfamilies (A-, M-, O-, P-, S-, and T superfamilies).[1] Among all of the conotoxins known to date, α-conotoxins of the A superfamily are the smallest in size, and they form one of the most extensively studied classes of conopeptides.

α-Conotoxins are short peptide toxins containing 12−19 amino acid residues with two disulfide bridges formed from the four conserved cysteine residues. As a consequence of these highly constraining disulfide linkages, the peptide backbone is demarcated into two distinct loop regions. Based on the number of residues within the first and second intercysteine loops, α-conotoxins are further categorized as α3/5 family, α4/6 family, α4/7 family, and more recently, α4/4 family.[1,2] Despite these structural variations, α-conotoxins block nicotinic acetylcholine receptors (nAChR). However, α3/5-conotoxins are selective blockers of neuromuscular (or peripheral) nAChR, whereas α4/X-conotoxins are selective blockers of neuronal nAChR (except α-conotoxin EI).[1,3] The specificity of the α-conotoxins is not limited to the subclasses of nAChR but down to the specific subunit pairing of the pentameric channel structure. For example, ImI 4/3 α-conotoxin is specific for α7 subunit,[4] PnIB 4/7 α-conotoxin is specific for α3β2 nAChR,[5] and BuIA 4/4 α-conotoxin can kinetically discriminate β2 and β4 subunits of nAChR.[2] However, members of the α3/5- and α4/X-conotoxins have also been shown to exhibit similarity in their secondary structure within each family, forming distinct fold topologies.[6] The conserved structural features are the likely explanation for the specificity of the toxins to their target receptor sites. As such, α-conotoxins are increasingly being used as selective probes for specific nAChR subclasses.[6]

Until recently, all conotoxins possessing the similar quadruple cysteine framework were thought to fold preferentially toward the globular conformation and conserved disulfide bonds (C_{1-3}, C_{2-4}) with absolute fidelity.[3,6−17] Conotoxin analogues regiospecifically synthesized with non-native disulfide linkages showed variation in their biological properties. For example, the ribbon isoform (C_{1-4}, C_{2-3}) of α-conotoxin GI displayed a 10-fold reduction in activity.[18] In contrast, the non-native isoforms of AuIB α-conotoxin revealed a 10-fold increase in its inhibitory effect on nAChR as compared to the native globular form.[19] This highlights the importance of the disulfide linkages and the structural framework for the activity of this class of conotoxins.

Recently we purified and characterized CMrVIA, a novel conotoxin from the venom of *Conus marmoreus*.[20] It represents one of the three currently known members of the novel class of χ/λ-conotoxin.[20−22] The almost concurrent discovery of the same peptide toxin by two separate laboratories resulted in the dissimilar classification of these peptides as λ- and χ-conotoxin, respectively. Sequence alignment and comparison of disulfide connectivity have suggested that they, in fact, belong to the same conotoxin class. For example, the conopeptide with the sequence

* Corresponding author. E-mail: dbskinim@nus.edu.sg. Tel: +65 65165235. Fax: +65 67792486.

† Department of Biological Sciences, National University of Singapore.

‡ Department of Pharmacy, National University of Singapore.

§ Present address: 206 Sugar Hall Department of Basic Pharmaceutical Sciences College of Pharmacy University of Louisiana at Monroe Monroe, LA 71209-0470.

10.1021/bm060269w CCC: $33.50
Published on Web 07/11/2006

NGVCCGYKLCHOC had been independently discovered and termed as CMrVIB λ-conotoxin,[20] mr10a conopeptide,[21] and subsequently MrIA χ-conotoxin.[22] The combined nomenclature of χ/λ-conotoxin is used in this paper so as to acknowledge both nomenclatures. We have retained the nomenclature of "CMrVIA" χ/λ-conotoxin instead of "MrVIA" χ/λ-conotoxin, so as to prevent confusion with a structurally and functionally distinct conopeptide identified as μO-MrVIA conotoxin.[23,24]

Although possessing a similar conserved cysteine spacing and arrangement observed in the α-conotoxins, native χ/λ-conotoxins possess an alternate disulfide linkage pattern (C_{1-4}, C_{2-3}). Thus, they exhibit ribbon conformation as the native conformation in contrast to α-conotoxins. χ/λ-Conotoxins bind to a distinct set of receptors and hence possess different biological activities as a consequence of their dissimilar intercysteine loops and native conformations. The physiological targets of the amidated analogues of MrIA and MrIB χ/λ-conotoxins were identified to be a noradrenaline transporter instead of nAChR seen in the case of α-conotoxins.[22] As with α-conotoxins, native disulfide linkages and conformation are important for the biological potency of the χ/λ-conotoxins. We have shown that the chemically synthesized CMrVIA χ/λ-conotoxin with globular conformation exhibits more than 1000-fold reduction in seizure induction effects as compared to the native ribbon conformation.[20] Despite the advancing knowledge in the binding and function of the α- and χ/λ-conotoxins, the mechanisms and key structural elements which led to such biased folding tendency remain to be elucidated. This is especially intriguing, considering the hypervariability of sequence present in the two intercysteine loops, particularly in α-conotoxins.[25,26]

As a first step to a better understanding of the structural features which underlie the folding nature of the mature peptides from the two conotoxin families, we focused on the structural examination of an identified χ/λ-conotoxin. This will facilitate subsequent structural analysis and comparison with members of the α-conotoxin family. Although solution structures of α-conotoxin analogues with the ribbon conformation have previously been determined, the three-dimensional structure for the novel class of χ/λ-conotoxin remains to be established. Sharpe et al. and Nilsson et al. have earlier determined the amidated analogues of MrIB χ/λ-conotoxin and MrIA χ/λ-conotoxin, respectively, by NMR spectroscopy.[22,27] However, all three currently identified members of χ/λ-conotoxin were noted to possess a free carboxylic acid at their C-terminal ends; a distinct difference from the almost invariably conserved C-terminal amidation noted in α-conotoxin. We have shown earlier that C-terminal modifications in ImI conotoxin can have severe implications on its in vitro folding propensity.[28] Herein, we report the solution NMR structure and structural analysis of the native ribbon form of CMrVIA, as well as its non-native globular isoform.

Materials and Methods

Peptide Synthesis and Purification. Linear and selectively deprotected analogues of CMrVIA χ/λ-conotoxin were synthesized using solid-phase peptide synthesis on an ABI Pioneer model 433A Peptide Synthesizer using 9-fluorenylmethoxycarbonyl (Fmoc) chemistry. The peptides have a sequence of VCCGYKLCHOC-*COOH*. The synthetic peptides were assembled on a pre-loaded Fmoc-L-Cys(Trt)-PEG-PS (4-hydroxymethylphenoxyacetic acid linker) support resin, which cleaves to give a free carboxylic acid at the carboxyl terminus. Amino acid residues were coupled using *O*-(7-azabenzotriazol-1-yl)-1,1,3,−3-tetramethyluronium hexafluorophosphate/ *N*,*N*-diisopropylethylamine in situ neutralization chemistry. The assembled peptides were then cleaved off the resin using a cocktail of 90% trifluoroacetic acid (TFA), 4% 1,2-ethanedithiol, 4% thioanisole, and 2% water. The crude peptides were purified on a Phenomenex Jupiter 300 Å 5 μ C18 (10 mm × 250 mm) semipreparative column on a ÄKTA purifier system to >90% purity before lyophilization. The fully deprotected and reduced peptides were verified using ESI-MS prior to folding studies by air oxidation in the folding buffer (100 mM Tris-HCl and 2 mM EDTA, adjusted to pH 8.5) at a concentration of 0.1 mM of peptide and allowed to stir in air for 48 h.

Orthogonal protection of cysteine residues' side chain functional group was used to generate specific disulfide isoforms of interest. Cysteine residues involved in the formation of the first disulfide bridge were protected with TFA-labile S-Trityl group, while the remaining two cysteine residues were protected by *S*-acetamidomethyl side chain protection group. Essentially, a two-step oxidation strategy was employed to obtain regiospecifically synthesized structural isoforms. The first pair of cysteine residues was deprotected in the resin-cleavage steps and allowed to oxidize freely in air by stirring in 0.1 M ammonium bicarbonate (pH 8.5) for 48 h at a peptide concentration of 0.1 mg/mL. Formation of the first disulfide bridge was verified by the reduction of two mass units in the oxidized product. The second disulfide bridge was formed by adding 0.1 M I_2 to a deaerated solution containing 0.1 mM peptide (10 equivalent/ACM) in acetonitrile/TFA/water (20:2:78% v/v), and stirred vigorously under nitrogen blanket for 5 min before quenching with 1 M ascorbic acid dropwise until the solution becomes colorless. Iodine oxidation was carried out in an acidic environment to ensure that there was no exchange of disulfide linkages. The oxidized peptides were then purified using RP-HPLC as described earlier.

NMR. CMrVIA conotoxin samples for NMR spectroscopy were prepared in 90% H_2O/ 10% D_2O to a concentration of 3−6 mM. 1D NMR of samples at peptide concentrations of 1, 3, and 6 mM were performed to ensure that no aggregation or peak broadening was noted at the various concentrations used. The pH of the dissolved peptide sample was then adjusted to 3.0 using deuterated hydrochloric acid or sodium hydroxide. All NMR experimental data including 1D ^{1}H NMR, 2D TOCSY, NOESY, and ROESY experiments were performed on a Brüker AVANCE DRX 500 MHz spectrometer with GRASP-II facility, complete with BVT 3000 control unit, capable of maintaining the temperature within ±0.1 K. NOESY and ROESY spectra were acquired at 200, 300, and 400 ms mixing times. Water suppression in the 2D spectra was achieved using a modified watergate sequence.[29] Spectra were acquired with 2048 and 512 data points in F2 and F1 respectively, processed with squared sine bell window functions shifted by 90°, before zero-filling to 2048 by 1024 data points. 1D ^{1}H NMR was carried out from 290 to 310 K at intervals of 5 K. Temperatures providing the optimal 1D spectra separation were used for subsequent 2D experiments. Temperature coefficients of the amide proton chemical shifts were derived from the 1D ^{1}H NMR spectra acquired over different temperatures. $^3J_{HN\text{-}H\alpha}$ coupling constants were derived from the 1D spectrum. All spectra were then analyzed using Mestres-C v: 4.5.2.0 software on Microsoft Windows platform.

Structure Calculation. Molecular modeling was done as per described in earlier literature.[28] Structure calculation was performed using InsightII 2000 software (Accelrys Inc. San Diego, CA) on an Origin 2000 Silicon Graphics computer. A consistent valence force field (Cvff) was used to calculate the conformational space consistent with the experimental ROE constraints derived from the NMR spectrum were examined in vacuo. ROE constraints were derived from the ROE peak volumes from the 300 ms ROESY spectra, and were classified as strong (1.9−3.1 Å), medium (1.9−3.8 Å), and weak (1.9−5.0 Å). The protons were brought to observable ROE distances using a penalty force of 100 kcal mol^{-1} Å^{-2}.

A distance versus time plot between the thiol groups of the four cysteine groups was generated after the initial round of energy minimization and dynamics at 300 K. The conformation with the shortest distance between the two pairs of cysteines corresponding to the ribbon conformation was manually bridged to form the two disulfide

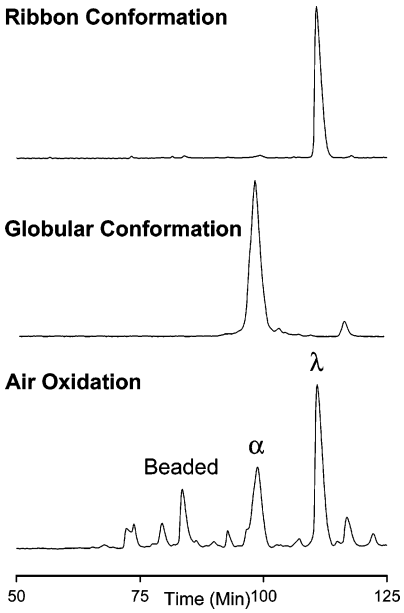

Figure 1. Chromatographic analysis of air oxidation products. Retention time of the three monomeric peaks in the elution profile of CMrVIA χ/λ-conotoxin formed from air oxidation were compared with that of regiospecifically synthesized globular and ribbon forms.

bonds. The potential of the resultant molecule was subsequently fixed before subjecting to further molecular modeling. High-temperature molecular dynamics was then performed using InsightII Discover module at 300 and 600 K at 10 ps, followed by 900 K at 20 ps with trajectories updated every 100 fs. All peptide bonds (except hydroxyproline residue) were tethered and held in the trans position with 100 kcal prior to the start of each high-temperature simulation. Simulated annealing was then performed by decreasing temperatures from 900 to 400 K at 10 ps in steps of 100 K before cooling to 300 K by "soaking" in an assembly of water molecules for 20 ps (sphere radius of 8 Å). Pseudo-atom corrections were made for methyl and methylene protons according to Wuthrich et al.[30] A total of 211 structures were generated, of which, the 15 frames with the lowest energy levels were relaxed using steepest descent method by subjecting to 100 steps of energy minimization, followed by conjugate gradient until the root-mean-square derivative was less than 0.6 kcal mol^{-1} Å. The final structure was then overlaid with the averaged structure of all 211 frames.

Results

Oxidation and Identification of Isoforms. Linear χ/λ-conotoxin CMrVIA (VCCGYKLCHOC-*COOH*) was chemically synthesized by solid-phase peptide synthesis utilizing Fmoc chemistry. The peptide was then purified to >90% using RP-HPLC and characterized by mass spectrometry. The observed mass of 1241.4 ± 0.6 Da corresponds well with the theoretical mass of 1241.6 Da.

Earlier work with α-conotoxins and χ/λ-conotoxins have utilized a variety of in vitro folding environments.[19,22,31,32] In this case, oxidation studies of reduced CMrVIA conotoxin were conducted in folding buffer comprising of 100 mM Tris Cl and 2 mM EDTA, maintained at pH of 8.5. As expected, CMrVIA conotoxin folds to give three monomeric isoforms, and these isoforms were resolved on a RP-HPLC C18 analytical column (Figure 1). Products in each peak were verified to contain the oxidized peptide as determined by the reduction of 4 mass units corresponding to the formation of two disulfide bridges (Figure 2). The beaded form, globular form, and the ribbon conformation sequentially eluted on the RP-HPLC chromatogram, and the amounts for these three structural isoforms were in proportions

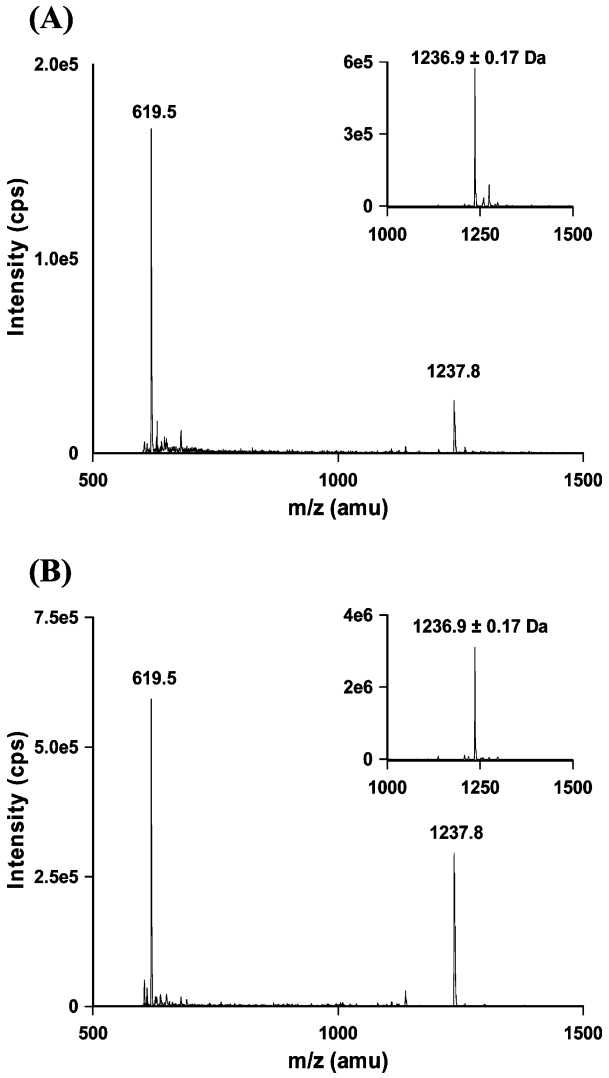

Figure 2. Molecular mass determination of (A) CMrVIA χ/λ-conotoxin globular conformation and (B) CMrVIA χ/λ-conotoxin ribbon conformation. Mass spectrums for the peptides were acquired on an electrospray-ionization mass spectrometer.

of 16:31:53, respectively. The globular and ribbon form of CMrVIA conotoxin were also regiospecifically synthesized by means of a two-step selective deprotection scheme. The synthesized ribbon form is indistinguishable from the major isoform (third peak of chromatogram) in terms of peak shape and chromatographic retention time. The non-native globular form coelutes with second major isoform (second peak of chromatogram) (Figure 1).

NMR Spectroscopy. To verify the structural identities of the isoforms obtained from the air oxidation of CMrVIA χ/λ-conotoxin, 1D ^{1}H NMR was performed for the peptides obtained from all three peaks obtained from the chromatogram. As with the coelution profiles, the 1D NMR spectra for the second and third peaks from the chromatogram were identical to that of the regiospecifically synthesized globular and ribbon conformations, respectively (Figure 3). 2D NMR experiments and structure calculations were performed on the purified regiospecifically synthesized isoforms upon verification of conformation as described earlier.

1D ^{1}H NMR was also conducted at various temperatures between 290 and 310 K. 1D NMR spectra for both samples were well resolved at all of the temperatures used, with amide chemical shifts spanning the range of 8.2−9.2 ppm. Based on the results, the optimal temperature for 2D ^{1}H NMR spectros-

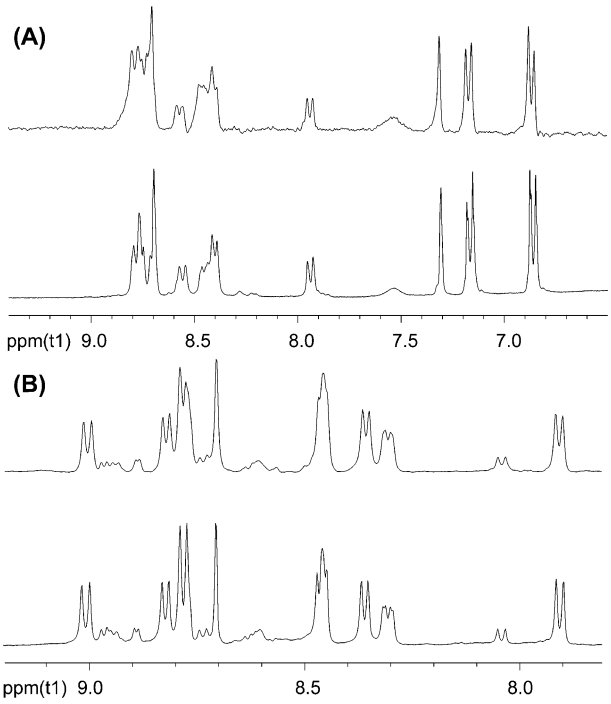

Figure 3. Comparison of 1D ^{1}H NMR spectra of CMrVIA χ/λ-conotoxin conformers. Panel A represents the ribbon isoform of CMrVIA χ/λ-conotoxin, and panel B represents the globular isoform, compared with the oxidized products of the chromatographic peaks which coelutes at the same retention time.

copy of the two samples was determined. Both 2D NOESY and ROESY experiments were performed on the peptide samples. Although the overall spectra for both sets of experiments were similar, the NOESY spectra suffered weaker intensity in the αH−βH region (Supporting Information). As such, ROESY experiments were used for the structural analysis of the peptides. The 2D NMR ROESY and TOCSY spectra of native CMrVIA χ/λ-conotoxin and its globular isoform were determined at 300 and 295 K respectively (Figure 4).

Native Ribbon Conformation. Earlier, we have shown that native CMrVIA χ/λ-conotoxin bears an identical disulfide linkage and chromatographic coelution profile with the regiospecifically synthesized ribbon conformation.[20] In this work, we examined the solution conformation of the synthesized ribbon conformation. The ribbon conformation of CMrVIA χ/λ-conotoxin bearing the C_{1-4}, C_{2-3} disulfide linkage yielded 2D NMR spectra of good quality, with reasonable dispersion of amide chemical shifts. This is indicative of a defined structure for the peptide molecule. Figure 4A shows the assignment of the various spin systems in the TOCSY spectrum, as well as the sequential assignment in the fingerprint region of the ROESY spectrum. Sequential connectivity of the various spin-systems was established based on strategies described elsewhere.[19,22,30−32]

A total of 91 ROEs were obtained from the 2D NMR spectra. Of these, 19 were sequential ROEs, 60 were intraresidue ROEs, and 12 were medium/long-range ROEs (Figure 5A). A strong ROE between His9 αH and Hyp10 δH suggests a trans peptide bond between these two residues. The identification of ROEs between Cys2 βH to Cys12 αH and Cys2 βH to Cys12 βH (Figure 4C) verifies the C_{1-4}, C_{2-3} disulfide connectivity characteristic of the ribbon conformation. All Cβ protons (except Cys3) of the various spin systems were also well resolved, indicative of well-defined side chain orientation for the residues. Except for the amide of His9, all other residues possess temperature coefficients of <-4 δppb/ K, indicating solvent exposure of amide protons for these residues (Figure 5C). Positive deviation of αH chemical shift index was observed for the regions between Cys2−Gly4 and Leu7−Hyp10. For small peptides such as these, it is usually difficult to observe stable β-sheet structures. Therefore, the positive deviation of chemical shifts from the random coil structure is suggestive of a stable secondary structure between these residues (Figure 5D).

Globular Conformation. The non-native globular conformation of CMrVIA χ/λ-conotoxin yielded 2D NMR spectra with a well-dispersed chemical shift in the amide region. However, unlike the earlier spectrum for the ribbon conformation, the globular form showed the presence of a minor conformation, almost 20% of the major conformation (Figure 4B). Adulteration of the sample by contaminants is eliminated, as determined using HPLC as well as ESI-MS.

It is interesting to note that in the case of GI α-conotoxin, it is the non-native ribbon conformation but not the native globular conformation that showed the presence of minor conformers.[18] Due to the small number of cross-peaks for the minor form, sequential assignment was only performed for the major conformer of globular CMrVIA conotoxin. Of the 103 ROEs observed for the major conformation, 25 were sequential, 68 were intraresidue, and 10 were medium/long-range ROEs (Figure 5B). Although the CβH−CβH ROE for Cys2−Cys8 and Cys3−Cys11 could not be identified, the presence of Gly4 αH to His9 δH ROE, Cys3 βH to Cys11 NH ROE, and Cys2 βH to Leu7 NH ROE (Figure 4D) is indicative that the disulfide connectivity for this isoform is irrevocably the C_{1-3}, C_{2-4} cysteine linkage observed in the globular framework. The low-temperature coefficients for Cys3 and Leu7 are indicative of solvent-shielding and intramolecular hydrogen bonding (Figure 5C). This corresponds well with the final molecular model in which these two residues are hydrogen bonded to Leu7 and Tyr5, respectively. As with the ribbon conformation, a strong ROE between His9 αH and Hyp10 δH was also observed in the globular form, suggesting a similar trans peptide bond. As the sequential connectivity of the minor conformer could not be established, the likelihood of cis−trans isomerization of Hyp9 attributing to the formation of an additional conformer could not be eliminated. Mass spectrometry data, HPLC elution profiles, and 1D ^{1}H NMR at variable temperature between 283 and 323 K further suggest that the additional minor spin systems noted in the spectra were unlikely to be derived from contamination in the NMR samples. From the NMR data, local structuring was also not as well defined for the globular form. This can be seen from the αH chemical shift index, from which no definitive clusters of deviation can be noted (Figure 5D).

Despite the identical amino acid sequence, the differences in 2D NMR spectra for the two isoforms could be observed, emphasizing the differing conformation presented. Cys3 amide proton which had a more upfield chemical shift of 8.8 ppm in the native form was seen to be more downfield (9.0 ppm) in the non-native globular conformation. In contrast, residues G4, Y5, and C8 were seen to move upfield by ∼0.1 ppm in the non-native form.

In earlier work comparing the native globular and non-native ribbon conformation of GI α-conotoxin,[18] the differences in spectra between the isoforms of the same sequence were much more drastic. This is unlike the lower scale of disparity noted between the two conformations of CMrVIA conotoxin which presumably, could be attributed to the smaller second intercysteine loop size (2 residues in CMrVIA χ/λ-conotoxin as compared to 3−7 residues in α-conotoxin) and presence of a

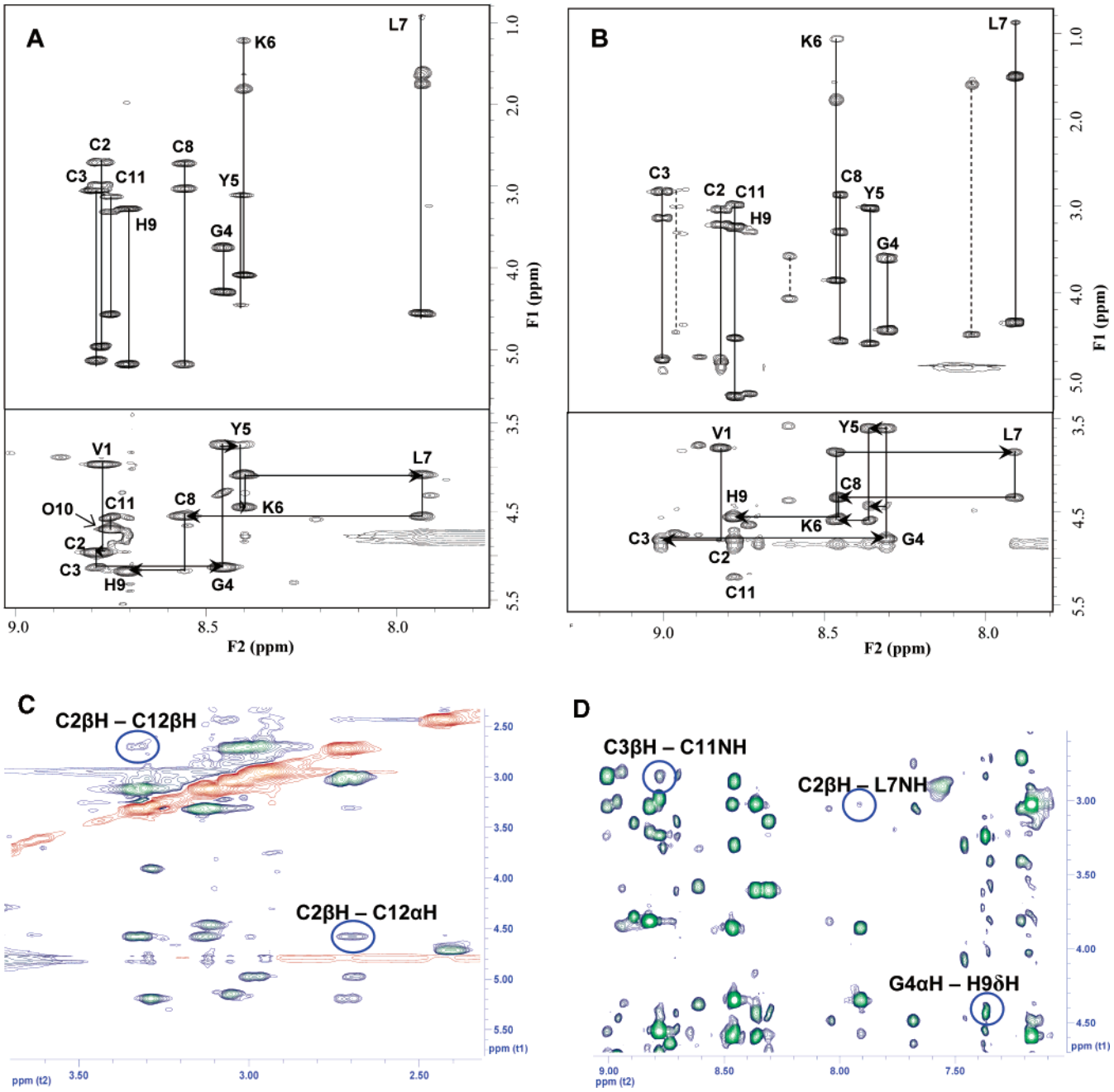

Figure 4. 2D ^{1}H NMR Spectra comparison. Figure summarizes the TOCSY (top panel) and ROESY (bottom panel) for the amide region of (A) ribbon conformation and (B) globular conformation. (- - -) represents spin systems arising from minor conformer(s). Panels C and D highlight the crucial ROEs verifying the canonical structures observed in the ribbon and globular conformation, respectively.

conserved hydroxyproline and the consequent lower level of flexibility. [20]

Structural Calculation. The final three-dimensional structures were calculated from the distance constraints derived from the peak volumes of ROE cross-peaks of ROESY spectra. In both the conformations examined, the averaged conformations were calculated from the 211 structures generated from the trajectory analysis of molecular dynamic simulation. This averaged conformation was chosen to represent the final calculated structure. The 15 structures with the lowest energy level were overlaid to represent the ensemble of the solution conformation of the final calculated structure. A summary of statistics for the structural calculation is shown in Table 1.

For the native ribbon conformation of CMrVIA conotoxin, pairwise comparison of the backbone for the 15 final calculated structures with the averaged structure gave a RMSD of 0.48 ± 0.1 Å. Superposition of heavy atoms from the structures gave a RMSD of 0.65 ± 0.1 Å, whereas all atom overlay had a RMSD of 0.81 ± 0.1 Å. The final averaged structure calculated had one ROE violation of less than 0.3 Å, and three violations of greater than 0.3 Å. Except for Hyp and Gly residues, 45.5% of all other residues fell within the allowed region, whereas the remaining 54.5% resided in the additionally allowed region of the Ramachandran plot.

The converged calculated solution structure for the globular conformation had a backbone RMSD of 0.58 ± 0.1 Å, heavy atom RMSD 0.76 ± 0.2 Å, and an all atom overlay RMSD of 0.91 ± 0.3 Å. These results were inline with the NMR spectra, from which the flexibility of the molecule could also be inferred from the presence of a minor conformer. Aside from glycine and hydroxyproline residues, 44.4% of the remaining residues were in the fully allowed region, 45.6% in the additionally

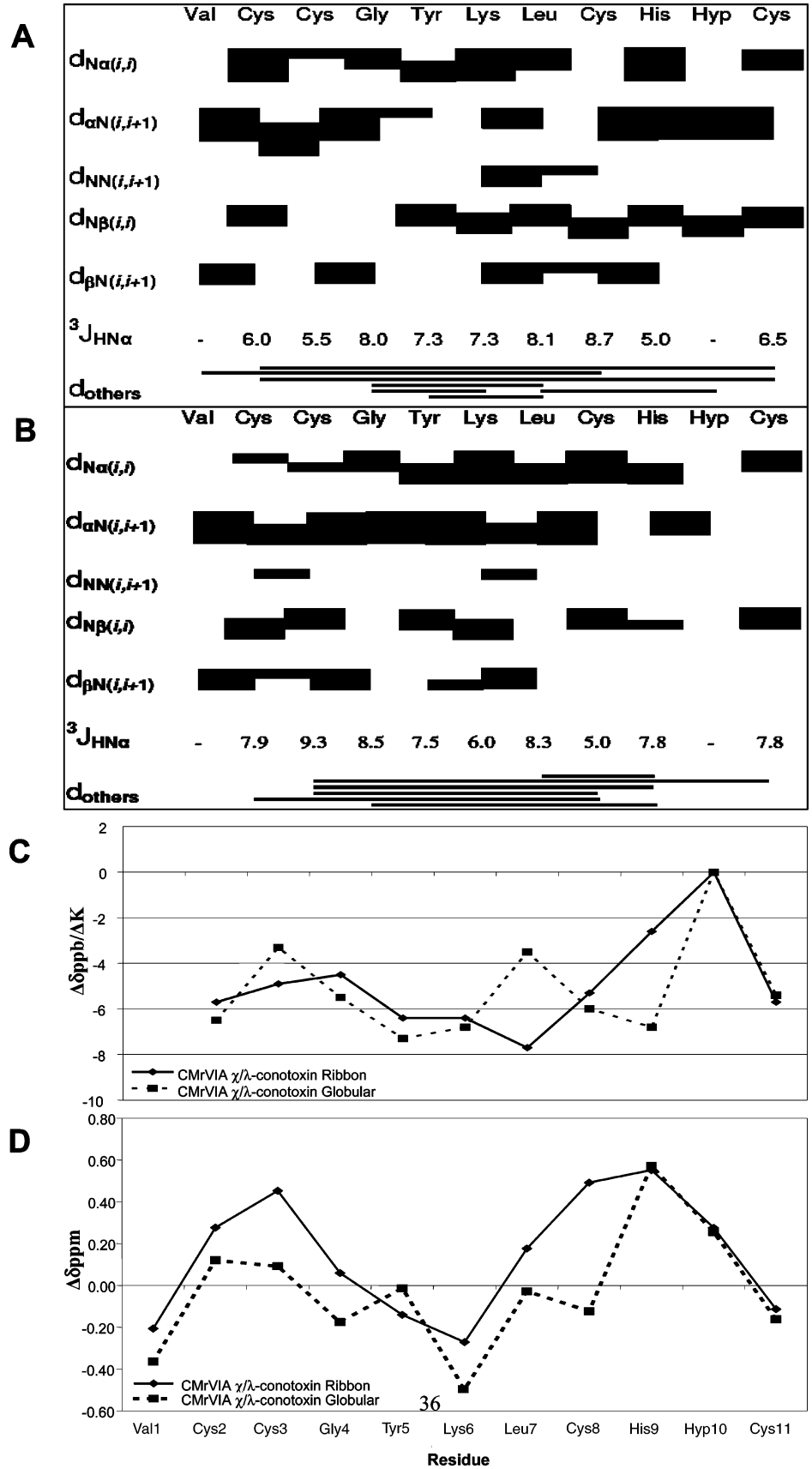

Figure 5. Summary of 2D NMR data. Sequential ROE data, $^3J_{HN\text{-}H\alpha}$ coupling constants, as well as medium and long-range ROEs for CMrVIA χ/λ-conotoxin ribbon conformation and globular conformation are presented in panels A and B, respectively. The relative intensity of ROEs in the 2D ROESY spectra (weak, medium, and strong) are depicted by the relative thickness of the bars. ROE between His9 CαH and Hyp10 CδH is indicated in diagram as a gray shaded box. ROE lines presented under d_{others} refer to the miscellaneous ROEs between any protons of the residues at the two ends of the lines. Panel C presents the temperature coefficient of amide chemical shifts for the respective residues in the two isoforms. Panel D summarizes the deviation of experimental Cα protons chemical shift values from random coil chemical shift values for the respective amino acids in both the CMrVIA χ/λ-conotoxin isoforms.

Table 1. Structural Statistics for Calculated Structures

	ribbon conformation	globular conformation
total number of constraints	91	105
intraresidue	60	64
short range (distance |i−j| =1)	20	30
medium range (distance 1<i≤ 2)	4	3
long range (distance > 2)	7	8
Ramachandran plot regions[a]		
% in favored region	45.5	44.4
% in additionally allowed region	54.5	45.6
% in generously allowed region	0.0	10.0
% in generously allowed region	0.0	0.0
NOE violations		
number of violations < 0.3 Å	1	2
number of violations > 0.3 Å	3	0
atomic root-mean-square with mean structure		
all atom RMSD	0.81 ± 0.1	0.91 ± 0.3
backbone RMSD	0.47 ± 0.1	0.58 ± 0.1

[a] Ramachandran plot regions calculated based on nonglycine and non-hydroxyproline residues.

allowed region, and 10% in the generously allowed region of the Ramachandran plot.

Cys11 of χ/λ-conotoxin CMrVIA forms a disulfide bridge with Cys2 and Cys3 in the ribbon and globular conformation, respectively. Unlike α-conotoxins which have three or more residues residing between the third and fourth cysteine residue of the conserved cysteine framework, χ/λ-conotoxins possesses a comparatively less flexible second intercysteine loop with only two residues in the same region. This was compounded with the presence of a hydroxyproline residue. These facts possibly contribute to the relatively lower percentages of residues residing in the fully allowed region of the Ramachandran plot.

The ensemble of structures for both the ribbon and globular conformation of χ/λ-conotoxin CMrVIA have been deposited into the Protein Data Bank (PBD ID 2B5P and PDB ID 2B5Q, respectively)

Description of the Structure of Isoforms. Figure 6A shows the backbone superposition of the 15 calculated solution structures for the ribbon conformation. The native isoform has a flat and ribbonlike backbone possessing a β turn as the predominant secondary structural element. The C-termini of the molecule is tethered close to the N-termini as a consequence of the restraining Cys2−Cys11 disulfide linkage. The side chains of most residues protrude freely into the solvent. The overall conformation is essentially formed by a turn between Gly4−Cys8 as dictated by the disulfide bridge cross-linking Cys3−Cys8. However, the loose turn observed within this nonhelical pentapeptide region has a distance of more than 7 Å between C^{α}(i) and C^{α}(i+4) residues, and lacks the characteristic supporting hydrogen bonds maintaining the tight turn observed in α or β turns. Φ and ψ angles for the residues in this segment were also beyond ±40 ° of the dihedral angles observed in standard β turns.

The superposition of the ensemble 15 final structures for the globular conformation of χ/λ-conotoxin CMrVIA is shown in Figure 6B. Unlike the native ribbon conformation, the amino and carboxyl termini of the globular form are distant in space, attributed to the two crossed disulfide bridges demarcating the

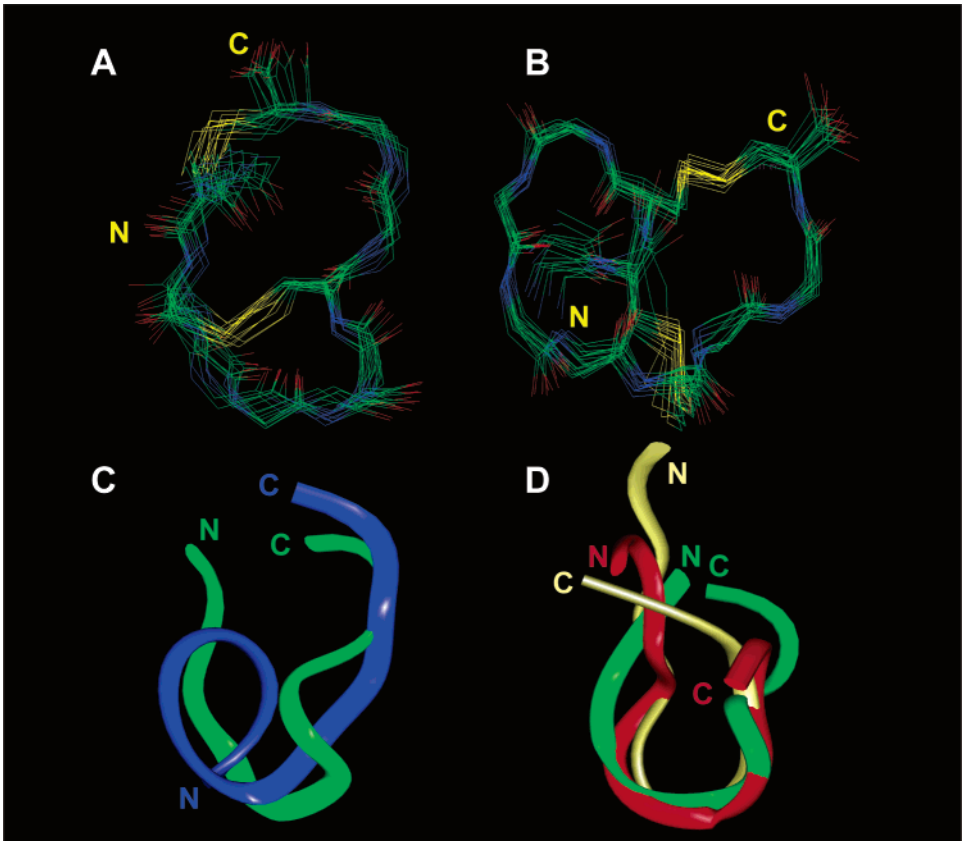

Figure 6. Structural analysis of conformers. The backbone superposition of the 15 final structures for (A) ribbon conformation and (B) globular conformation for CMrVIA χ/λ-conotoxin. Panel C shows the backbone superposition of globular (blue) and ribbon conformation (green) of CMrVIA conotoxin. Panel D illustrates the structural overlay of MrIB-NH_2 structure (red), MrIB-NH_2 structure (white), with the native ribbon conformation of CMrVIA χ/λ-conotoxin (green), aligned along residues Gly4−Cys8 of the latter peptide.

intercysteine loops. The amide proton of Cys2 forms a tight intraturn hydrogen bond with the carbonyl group of Tyr5. The resultant β turn formed between Cys2−Tyr5 of the first intercysteine loop is reinforced with a further intraturn hydrogen bond between Cys3 and Gly4, forming a typical Type II β turn. The distance of C_α carbon of Cys2 (C_i) to Tyr5 (C_{i+3}) of the β turn measures at 6.2 Å. The first disulfide bridge formed between Cys2 and Cys8, as well as additional noncovalent interactions between Cys3 and Tyr5 with the remaining residues of the first intercysteine loop pegs the turn closely to the peptide backbone into almost a helix-like turn. The remaining backbone segment between Leu7−Cys11 forms a relatively linear conformation. Interestingly, the globular form lacks any of the helical segments observed in the similar structural isoform of native α-conotoxins.

Neuronal nAChR specific α-conotoxins (ImI, EpI, PnIA, PnIB, and MII conotoxin) share a common ω-shape local backbone conformation and rigid hydrophobic core.[33] Despite the presence of identical disulfide linkage patterns with native α-conotoxins, the regiospecifically synthesized globular form of χ/λ-conotoxin CMrVIA lacks the ω-shaped molecular backbone common to 4/7 α-conotoxins. The absence of crucial supporting hydrogen interaction as well as the proline residue in position 6 of non-native conformation of χ/λ-conotoxin CMrVIA may have resulted in the loss of the 3_{10}-helical turn, characteristic of the α-conotoxin fold.[33,34]

Discussion

χ/λ-Conotoxins are novel peptide toxins isolated from the venom of the marine predatory cone snails. Despite possessing the conserved cysteine framework seen in α-conotoxins, the disulfide bonding patterns and biological activities of these two classes of conopeptides are distinctly different: χ/λ-conotoxins possess the C_{1-4}, C_{2-3} disulfide pairing and they target noradrenaline transporter,[22] whereas α-conotoxins possess the C_{1-3}, C_{2-4} canonical form and target nicotinic acetylcholine receptors.[1] To lay the foundation for the comparison of the structure−function relationship of these two classes of conotoxins, it is crucial to elucidate the structural features of the ribbon conformer found native to χ/λ-conotoxins. Therefore, we have examined the structure of χ/λ-conotoxin CMrVIA isolated from *Conus marmoreus*.

In addition to the native ribbon form (C_{1-4}, C_{2-3}) in χ/λ-conotoxin, two other conformations are theoretically possible for the same sequence, namely the beaded form (C_{1-2}, C_{3-4}) and the globular form (C_{1-3}, C_{2-4}). These two forms, however, are not natively observed in the venom of *C. marmoreus*. The beaded isoform requires the formation of a vicinal disulfide bridge and is thermodynamically unfavorable. The non-native globular isoform is of particular interest, as this is the kinetically favored conformation in the closely related class of α-conotoxin. To understand the structural differences seen in these two classes of conotoxins possessing the respective dominant conformation, we have also examined the solution structure of the globular conformation of χ/λ-conotoxin CMrVIA.

The differences in structural features of the ribbon conformation (C_{1-4}, C_{2-3}) and the globular conformation (C_{1-3}, C_{2-4}) are evident from the final calculated conformations (Figure 6). The native ribbon conformation of CMrVIA χ/λ-conotoxin exhibits a loose turn, restrained through the formation of the two crucial disulfide linkages aligned almost in a parallel fashion in the final conformation of the peptide. The key structural element present in the globular conformation is a Type II β turn within the first intercysteine loop, positioned close to the nonhelical segment of the remaining peptide framework. Despite the identity in sequence, superposition of the ribbon with globular conformations of χ/λ-conotoxin CMrVIA revealed a paired-wise backbone RMSD of 4.72 Å (Figure 6C), emphasizing the distinctly different conformation of the non-native globular form as compared to the native ribbon conformation.

The solution structure for an amidated analogue of MrIB conotoxin (VGV**CC**GYKL**C**HO**C**-*CONH*$_2$, MrIB-*NH*$_2$), a member of χ/λ-conotoxin, was determined by Sharpe et al. using NMR spectroscopy.[22] The solution structure of the MrIB-*NH*$_2$ analogue was calculated to a precision of 1.23 Å (paired-wise backbone comparison) and was observed to have a flexible β-hairpin structure about Tyr7 and Leu9. MrIB-*NH*$_2$ was suggested to possess a minor conformer in its solution structure. The amino acid sequence of the native carboxylate form of CMrVIA χ/λ-conotoxin is essentially identical to the segment between Val3−Cys13 of MrIB-*NH*$_2$, less the modified amidated C-terminal. MrIB-*NH*$_2$, however, has two additional residues at the N-terminal. Despite the overlapping segments of the amino acid sequence and analogous C_{1-4}, C_{2-3} canonical disulfide linkages, the similarity of the final calculated solution structures for the two peptides were limited. Segments of MrIB-*NH*$_2$ corresponding to Val1−His9 of CMrVIA χ/λ-conotoxin overlaid with a paired-wise backbone RMSD of 2.52 Å. The backbone structure of the segment between Gly4−Cys8 of CMrVIA χ/λ-conotoxin is fairly similar to the segment between Gly6−Cys10 of MrIB-*NH*$_2$ conotoxin. Figure 6D illustrates the backbone superposition of MrIB-*NH*$_2$ with the ribbon conformation of CMrVIA χ/λ-conotoxin, aligned along the segment between residues Gly4−Cys8 of the latter molecule. These segments were calculated to overlay with an RMSD of 1.73 Å.

Recently, Nilssson et al. have also reported the solution structure of the amidated analogue of another member of χ/λ-conotoxin, called MrIA conotoxin (NGV**CC**GYKL**C**HO**C**-*CONH*$_2$, MrIA-*NH*$_2$).[27] The sequence of MrIA conotoxin matches closely with that of MrIB conotoxin, differing by a single residue at the N-terminus. Despite the high level of sequence similarity and disulfide connectivity, MrIA-*NH*$_2$ conotoxin had a surprisingly poor RMSD of 2.93 Å in the paired-wise backbone comparison with MrIB-*NH*$_2$ conotoxin. As with MrIB conotoxin, residues Val3-Cys13 of MrIA are identical to the sequence of CMrVIA χ/λ-conotoxin. However, these segments overlaid poorly with latter sequence, giving an RMSD of 3.11 Å (Figure 6D).

The comparison of reported structures between the closely related MrIB-*NH*$_2$ conotoxin, MrIA-*NH*$_2$ conotoxin, and subsequently CMrVIA χ/λ-conotoxin, suggest that the presence of the segments Val1-Gly2 and Asn1-Gly2 that are N-terminus to the sequence seen in CMrVIA χ/λ-conotoxin have important implication on final conformation of the peptide structures. These residues are likely to have steric or electrostatic effects on the final conformation of the peptide structures.

In small peptides, especially those possessing multiple disulfide bridges, and/or glycine or proline residues, the presence of multiple conformations within a single isoform is not uncommon. In earlier studies with α-conotoxin GI, heterogeneity of solution conformers was also observed for the non-native ribbon conformation. Considering the fact that CMrVIA χ/λ-conotoxin possesses a similar C_{1-4}, C_{2-3} disulfide-linkage pattern observed in the non-native form of α-conotoxin, the native ribbon conformation is surprisingly homogeneous. Only a single conformer is evident from the 2D NMR spectra, from which a single set of associated spin systems was identified. In

contrast, the globular conformation exhibits a higher degree of flexibility and conformational heterogeneity as compared to the ribbon conformation. This is despite the presence of a similar number of ROE cross-peaks in the NMR spectra for both conformations.

In earlier work by Gehrmann et al.,[18] it has been described that the precision of the calculated conformation of GI α-conotoxin is in the order of globular > ribbon > beaded. Complemented with the folding studies by Zhang and Synder,[35] the authors concluded that the conformational flexibility of the various isoforms correlate well with the thermodynamic stability as expressed by the percentage yield obtained from oxidation studies. The globular conformation of GI α-conotoxin, which had the lowest paired-wise backbone RMSD, had the highest yield of 71% from oxidation studies. In the case of CMrVIA χ/λ-conotoxin, the ribbon conformation yielded the highest percentage from an air oxidation study carried out under conditions similar to those cited by Zhang and Snyder.[35] Incidentally, the solution structure of the ribbon isoform of CMrVIA conotoxin was also calculated to a higher precision as compared to its non-native conformations. This suggests that the folding tendency of CMrVIA χ/λ-conotoxin could possibly an outcome of thermodynamic stability of the ribbon conformation as compared to the globular structural isoform.

Conclusion

We have presented the three-dimensional structures of the native ribbon conformation and the globular analogue of CMrVIA χ/λ-conotoxin. As in the case of α-conotoxins, the ribbon and globular forms exhibit significantly different solution conformations. By comparing the globular analogues between the two classes of closely related peptides, we have noted the role of key residues such as Pro6 residue that is seen conserved in α-conotoxins on the structural elements of the peptide backbone (unpublished observations). It is also interesting to note that, although the globular conformation of α-conotoxins has a more precise structure as compared to its ribbon non-native analogue, the converse is true for CMrVIA χ/λ-conotoxin which natively adopts the ribbon form. α-conotoxins have been suggested to represent potent and effective minimal functional protein, projected on an effective scaffold to topologically arrange the residue side chains for interaction.[6] By understanding the structure−function relationship of this unique class of peptide toxins, it would then be possible to harness the therapeutic potential of these potent and specific peptides.

Though the first χ/λ-conotoxin was identified over five years ago,[21] the specific structural features leading to the distinct folding patterns and consequent biological activities have barely been addressed. By aligning sequences of known χ/λ- and α-conotoxins, our group has recently identified the role of the conserved C-terminal amidation in the folding of ImI α-conotoxin.[28] Current work underway in our laboratory has also suggested the role of several other structural keys which play pertinent roles in the folding of these two structurally related families of peptide toxins (unpublished observations).

Acknowledgment. This work is supported by Biomedical Research Council, Agency for Science and Technology, Singapore. T.S.K. acknowledges the Singapore Millennium Foundation for granting the research scholarship. The authors thank the Chemical and Molecular Analysis Center, Department of Chemistry, and Protein and Proteomic Centre, Department of Biological Sciences at National University of Singapore for allowing the use of the NMR spectrometers and protein core facilities, respectively.

Supporting Information Available. 2D ^{1}H NMR ROESY and NOESY spectra and structures showing overlays of the different conformations. This material is available free of charge via the Internet at http://pubs.acs.org.

References and Notes

(1) McIntosh, J. M.; Santos, A. D.; Olivera, B. M. *Annu. Rev. Biochem.* **1999**, *68*, 59−88.
(2) Azam, L.; Dowell, C.; Watkins, M.; Stitzel, J. A.; Olivera, B. M.; McIntosh, J. M. *J. Biol. Chem.* **2005**, *280*, 80−87.
(3) Martinez, J. S.; Olivera, B. M.; Gray, W. R.; Craig, A. G.; Groebe, D. R.; Abramson, S. N.; McIntosh, J. M. *Biochemistry* **1995**, *34*, 14519−14526.
(4) Johnson, D. S.; Martinez, J.; Elgoyhen, A. B.; Heinemann, S. F.; McIntosh, J. M. *Mol. Pharmacol.* **1995**, *48*, 194−199.
(5) Luo, S.; Nguyen, T. A.; Cartier, G. E.; Olivera, B. M.; Yoshikami, D.; McIntosh, J. M. *Biochemistry* **1999**, *38*, 14542−14548.
(6) Janes, R. W. *Curr. Opin. Pharmacol.* **2005**, *5*, 280−292.
(7) Luo, S.; Kulak, J. M.; Cartier, G. E.; Jacobsen, R. B.; Yoshikami, D.; Olivera, B. M.; McIntosh, J. M. *J. Neurosci.* **1998**, *18*, 8571−8579.
(8) Loughnan, M. L.; Nicke, A.; Jones, A.; Adams, D. J.; Alewood, P. F.; Lewis, R. J. *J. Med. Chem.* **2004**, *47*, 1234−1241.
(9) Gray, W. R.; Luque, A.; Olivera, B. M.; Barrett, J.; Cruz, L. J. *J. Biol. Chem.* **1981**, *256*, 4734−4740.
(10) McIntosh, J. M.; Yoshikami, D.; Mahe, E.; Nielsen, D. B.; Rivier, J. E.; Gray, W. R.; Olivera, B. M. *J. Biol. Chem.* **1994**, *269*, 16733−16739.
(11) Cartier, G. E.; Yoshikami, D.; Gray, W. R.; Luo, S.; Olivera, B. M.; McIntosh, J. M. *J. Biol. Chem.* **1996**, *271*, 7522−7528.
(12) Loughnan, M.; Bond, T.; Atkins, A.; Cuevas, J.; Adams, D. J.; Broxton, N. M.; Livett, B. G.; Down, J. G.; Jones, A.; Alewood, P. F.; Lewis, R. J. *J. Biol. Chem.* **1998**, *273*, 15667−15674.
(13) McIntosh, J. M.; Dowell, C.; Watkins, M.; Garrett, J. E.; Yoshikami, D.; Olivera, B. M. *J. Biol. Chem.* **2002**, *277*, 33610−33615.
(14) Ellison, M.; McIntosh, J. M.; Olivera, B. M. *J. Biol. Chem.* **2003**, *278*, 757−764.
(15) Nicke, A.; Loughnan, M. L.; Millard, E. L.; Alewood, P. F.; Adams, D. J.; Daly, N. L.; Craik, D. J.; Lewis, R. J. *J. Biol. Chem.* **2003**, *278*, 3137−3144.
(16) Zafaralla, G. C.; Ramilo, C.; Gray, W. R.; Karlstrom, R.; Olivera, B. M.; Cruz, L. J. *Biochemistry* **1988**, *27*, 7102−7105.
(17) Fainzilber, M.; Hasson, A.; Oren, R.; Burlingame, A. L.; Gordon, D.; Spira, M. E.; Zlotkin, E. *Biochemistry* **1994**, *33*, 9523−9529.
(18) Gehrmann, J.; Alewood, P. F.; Craik, D. J. *J. Mol. Biol.* **1998**, *278*, 401−415.
(19) Dutton, J. L.; Bansal, P. S.; Hogg, R. C.; Adams, D. J.; Alewood, P. F.; Craik, D. J. *J. Biol. Chem.* **2002**, *277*, 48849−48857.
(20) Balaji, R. A.; Ohtake, A.; Sato, K.; Gopalakrishnakone, P.; Kini, R. M.; Seow, K. T.; Bay, B. H. *J. Biol. Chem.* **2000**, *275*, 39516−39522.
(21) McIntosh, J. M.; Corpuz, G. O.; Layer, R. T.; Garrett, J. E.; Wagstaff, J. D.; Bulaj, G.; Vyazovkina, A.; Yoshikami, D.; Cruz, L. J.; Olivera, B. M. *J. Biol. Chem.* **2000**, *275*, 32391−32397.
(22) Sharpe, I. A.; Gehrmann, J.; Loughnan, M. L.; Thomas, L.; Adams, D. A.; Atkins, A.; Palant, E.; Craik, D. J.; Adams, D. J.; Alewood, P. F.; Lewis, R. J. *Nat. Neurosci.* **2001**, *4*, 902−907.
(23) Fainzilber, M.; van der, S. R.; Lodder, J. C.; Li, K. W.; Geraerts, W. P.; Kits, K. S. *Biochemistry* **1995**, *34*, 5364−5371.
(24) McIntosh, J. M.; Hasson, A.; Spira, M. E.; Gray, W. R.; Li, W.; Marsh, M.; Hillyard, D. R.; Olivera, B. M. *J. Biol. Chem.* **1995**, *270*, 16796−16802.
(25) Conticello, S. G.; Gilad, Y.; Avidan, N.; Ben Asher, E.; Levy, Z.; Fainzilber, M. *Mol. Biol. Evol.* **2001**, *18*, 120−131.
(26) Olivera, B. M. *Mol. Biol. Cell* **1997**, *8*, 2101−2109.
(27) Nilsson, K. P.; Lovelace, E. S.; Caesar, C. E.; Tynngard, N.; Alewood, P. F.; Johansson, H. M.; Sharpe, I. A.; Lewis, R. J.; Daly, N. L.; Craik, D. J. *Biopolymers* **2005**, *80*, 815−823.
(28) Kang, T. S.; Vivekanandan, S.; Jois, S. D.; Kini, R. M. *Angew. Chem. Int. Ed Engl.* **2005**.
(29) Piotto, M.; Saudek, V.; Sklenar, V. *J. Biomol. NMR* **1992**, *2*, 661−665.
(30) Wuthrich, K. *NMR of Proteins and Nucleic Acids*; Wiley: New York, 1986.

(31) Gehrmann, J.; Daly, N. L.; Alewood, P. F.; Craik, D. J. *J. Med. Chem.* **1999**, *42*, 2364−2372.
(32) Bingham, J. P.; Broxton, N. M.; Livett, B. G.; Down, J. G.; Jones, A.; Moczydlowski, E. G. *Anal. Biochem.* **2005**, *338*, 48−61.
(33) Rogers, J. P.; Luginbuhl, P.; Shen, G. S.; McCabe, R. T.; Stevens, R. C.; Wemmer, D. E. *Biochemistry* **1999**, *38*, 3874−3882.
(34) Chi, S. W.; Kim, D. H.; Olivera, B. M.; McIntosh, J. M.; Han, K. H. *Biochem. J.* **2004**, *380*, 347−352.
(35) Zhang, R. M.; Snyder, G. H. *Biochemistry* **1991**, *30*, 11343−11348.

BM060269W